



doi:10.1016/j.gca.2003.09.016

## Raman spectroscopic study of CO<sub>2</sub>-NaCl-H<sub>2</sub>O mixtures in synthetic fluid inclusions at high temperatures

JINYANG CHEN,<sup>1,\*</sup> HAIFEI ZHENG,<sup>2</sup> WANSHENG XIAO,<sup>1</sup> YISHAN ZENG,<sup>2</sup> and KENAN WENG<sup>1</sup><sup>1</sup>Guangzhou Institute of Geochemistry, Chinese Academy of Sciences, Guangzhou 510640, China<sup>2</sup>Department of Geology, Peking University, Beijing 100871, China

(Received June 6, 2003; accepted in revised form September 16, 2003)

**Abstract**—Mixtures of CO<sub>2</sub>-NaCl-H<sub>2</sub>O contained in synthetic fluid inclusions are studied by laser Raman spectroscopy at high temperatures. With increasing temperature, the band splitting (X) of  $\nu_1$ - $2\nu_2$  diad of spectrum of CO<sub>2</sub> presents more variations, and the intensity ratios of the hot bands to the  $\nu_1$ - $2\nu_2$  diad increase. For mixtures of gas phase rich in CO<sub>2</sub> and liquid phase rich in H<sub>2</sub>O before homogenization, the strength of hydrogen bonding of water in the liquid phase decreases almost linearly with increasing temperature. When mixtures become homogeneous liquid phases, carbon dioxide content increases significantly as a result of the abrupt decrease in hydrogen bonds. Our results show that the hydrogen bonds change only slightly at higher temperatures above the homogeneous point, and a certain extent of the hydrogen bonds still remains at the highest temperature of 550°C of this work. The study is helpful to Raman spectroscopic analysis of natural fluid inclusions at high temperatures. Copyright © 2004 Elsevier Ltd

### 1. INTRODUCTION

Studies of hydrothermal fluids are important to understand phase equilibrium, dissolution, migration and deposition of mineral, abiogenic formation of oil and natural gas, geoelectric and geomagnetic discontinuity, and seismic wave (Duan et al., 2003; Xiao et al., 2001; Weng et al., 1999, 1997; Zheng et al., 1997; Seward et al., 1999). In addition, there are prospective applications to chemical engineering, material synthesis, disposal of hazardous waste, hydrometallurgy, desalination of seawater, and geothermal exploitation (Savage et al., 1995; Yamanaka et al., 2001; Ziegler et al., 2001; Daimon et al., 2001; Mitton et al., 2001; Kritzer and Dinjus, 2001). In recent years, with the development of high-temperature and high-pressure experimental technique and the applications of analytical instruments such as nuclear magnetic resonance (Hoffmann and Conradi, 1997; Matubayasi et al., 1997a, 1997b), X-ray diffraction (Ramos et al., 2000; Ohtaki et al., 1997), neutron diffraction (Okhulkov and Gorbaty, 2001; Ricci et al., 1998), microwave spectroscopy (Okada et al., 1997), X-ray absorption fine structure (Wallen et al., 1997, 1998; Seward et al., 1999; Bassett et al., 2000; Mayanovic et al., 2001; Anderson et al., 2002), Uv-vis (Suleimenov and Seward, 1997), infrared spectroscopy (Furutaka et al., 2001; Hu et al., 2000), and Raman spectroscopy (Frantz et al., 1993, 1994; Frantz, 1998; Fournier et al., 1998; Dubessy et al., 1999, 2001; Ebukuro et al., 1999; Walrafen et al., 1999; Ikushima et al., 1998a, 1998b; Carey and Korenowski, 1998; Carey et al., 1998), it is known that the strength of hydrogen bonding of water weakens with increasing temperature. At the critical point of pure water (374°C, 221 bar), the hydrogen bonds decrease abruptly. However, we have not sufficiently understood the nature of hydrogen bonding, and there are many arguments about whether they disappear or how many remain

at higher temperatures above the critical point (Postorino et al., 1993; Tromp et al., 1994; Hoffmann and Conradi, 1997; Gorbaty and Kalinichev, 1995; Matubayasi et al., 1997a, 1997b; Soper et al., 1997; Bellissent-Funel, 2001; Bellissent-Funel and Tassaing, 1997; Marti, 1999, 2000; Marti et al., 1996; Yamaguchi et al., 2001; Mayanovic et al., 2001). Furthermore, the effect of other species such as nondipolar molecules (CH<sub>4</sub>, N<sub>2</sub>, CO<sub>2</sub>) on the hydrogen bonding should be studied in detail.

CO<sub>2</sub>-NaCl-H<sub>2</sub>O is a typical geological fluid, and it is very important to geological processes in the deep earth. The properties of the hydrothermal fluid are closely related to the hydrogen bonding of water, for example, increasing temperature disrupts the hydrogen bonding and facilitates the insertion of CO<sub>2</sub>, and therefore increases its solubility. Raman spectroscopy is probably the most important of the techniques that have been employed to obtain information relating to the intra- and intermolecular vibrational modes of water. The stretching vibration ( $\nu_2$ ) of the Raman spectrum of water is sensitive to the hydrogen bonding (Frantz et al., 1993; Ikushima et al., 1998a); therefore, the aim of this paper is to characterize the modifications of the spectra of water of the CO<sub>2</sub>-NaCl-H<sub>2</sub>O system to give preliminary interpretations in terms of hydrogen bonds at high temperatures. In addition, the changes of spectra of CO<sub>2</sub> are examined in the prospective use of natural fluid inclusion analysis at high temperatures by micro-Raman spectroscopy.

Synthetic fluid inclusions give an ideal cell for high-temperature Raman spectroscopy. The scattering geometry used for synthetic fluid inclusions is similar to that of natural fluid inclusions; therefore, the results can be used for the analysis of natural fluid inclusions. Indeed, such an approach might be a good complement to classical optical cells for its unique geometry.

### 2. MATERIAL AND METHODS

Fluid inclusions were synthesized by healing fractures in natural quartz cores at various temperatures and pressures using the classical technique (Stern and Bodnar, 1984; Bodnar and Stern, 1985; Frost

\* Author to whom correspondence should be addressed (chenjy@gig.ac.cn).

Table 1. Forming temperatures and pressures, homogenization temperatures, and compositions of synthetic fluid inclusions.

Sample	T (°C)	P (MPa)	1	2	3	4
COHG	650	100	595.0–597.2	595.8 (8)	10% CO <sub>2</sub> + H <sub>2</sub> O	Gas
COHL	600	120	366.0–368.9	367.8 (7)	5% CO <sub>2</sub> + H <sub>2</sub> O	Liquid
SCOHL	600	120	399.1–402.0	400.5 (6)	5% NaCl + 5% CO <sub>2</sub> + H <sub>2</sub> O	Liquid
SCOHG	600	100	529.1–531.7	530.2 (7)	5% NaCl + 10% CO <sub>2</sub> + H <sub>2</sub> O	Gas

- (1) Range of measured homogenization temperatures (°C).
- (2) Average homogenization temperature (Th) (°C) and number of measurements (in parenthesis).
- (3) Composition in weight percent.
- (4) Phase of homogenization.

and Wood, 1997; Shmulovich and Graham, 1999; Bakker and Diamond, 2000; Schmidt and Bodnar, 2000). The CO<sub>2</sub> was obtained from the decomposition of Ag<sub>2</sub>C<sub>2</sub>O<sub>4</sub>. After the synthetic experiments, the quartz cores were cut into approximately 1-mm-thick disks, polished on both sides, and examined with a petrographic microscope. Almost all fluid inclusions distribute along the fractures of the quartz cores, and the liquid–gas ratios of every sample are almost equal, which indicates that fluid inclusions of every sample trapped a homogeneous fluid with the same composition and density as the parent solution (Sterner and Bodnar, 1984). The homogeneous temperatures (Th) of these samples were measured in Leitz 1350 stage. The forming temperatures and pressures, homogenization temperatures, and compositions of synthetic fluid inclusions are given in Table 1. Because the ranges of measured Th are less than 3°C, the results also confirm that the compositions and densities of the fluid inclusions of every sample are uniform.

Raman spectra were obtained by a Raman micro-spectrometer (RENISHAW System RM-1000, Renishaw group, Gloucestershire, United Kingdom) equipped with a heating stage (Linkam TM93). The measurements use an ionized Ar<sup>+</sup> laser,  $\lambda_0 = 514.5$  nm, 50 mW, entrance slit 50 nm, collection time 30 s, and range 1000–4000 cm<sup>-1</sup>. Cold water flowing through a copper tube, wound around the long-working-distance objective ( $\times 50$ , Olympus), allowed acquisition of spectra to 600°C without damaging the objective. Figure 1 clearly shows that mixtures of gas phase and liquid phase in fluid inclusions become homogeneous gradually during heating.

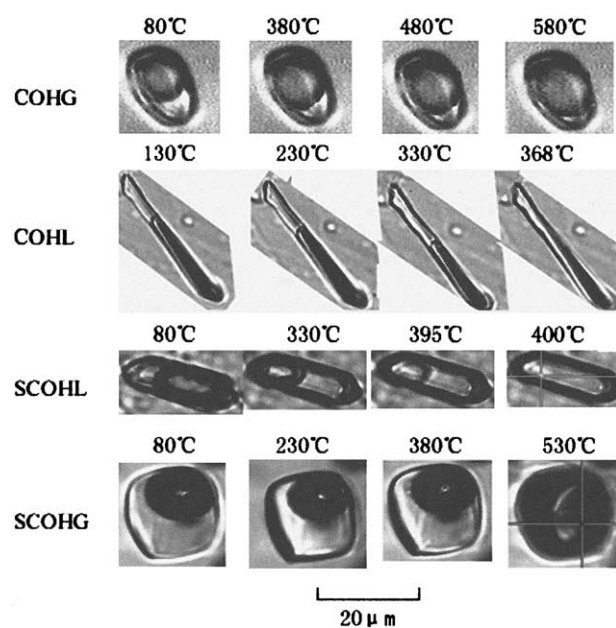


Fig. 1. Variation of mixtures in fluid inclusions during heating.

### 3. RESULTS

A typical Raman spectrum obtained from a synthetic fluid inclusion is illustrated in Figure 2a (SCOHG, gas phase: 330°C). At low wavenumbers, the bands of the quartz host crystal are identified, and they do not overlap with the bands of carbon dioxide and water.

Carbon dioxide exhibits two bands around 1380 and 1278 cm<sup>-1</sup> as results of Fermi resonance of  $\nu_1$  and  $2\nu_2$  (Wienecke et al., 1986; Rosso and Bodnar, 1995), and two obvious shoulder peaks called hot band near Fermi diad (Figs. 2 and 3). Before homogenization, the gas phase rich in CO<sub>2</sub> yields two strong bands of carbon dioxide, whereas the liquid phase rich in H<sub>2</sub>O gives two weak bands of carbon dioxide (Fig. 2b). In this study we discuss the strong bands of carbon dioxide obtained in gas phases only.

Figure 3 represents spectra of CO<sub>2</sub> in the gas phase of COHG (10%CO<sub>2</sub> + H<sub>2</sub>O, Th (G) = 596°C), and it shows that the

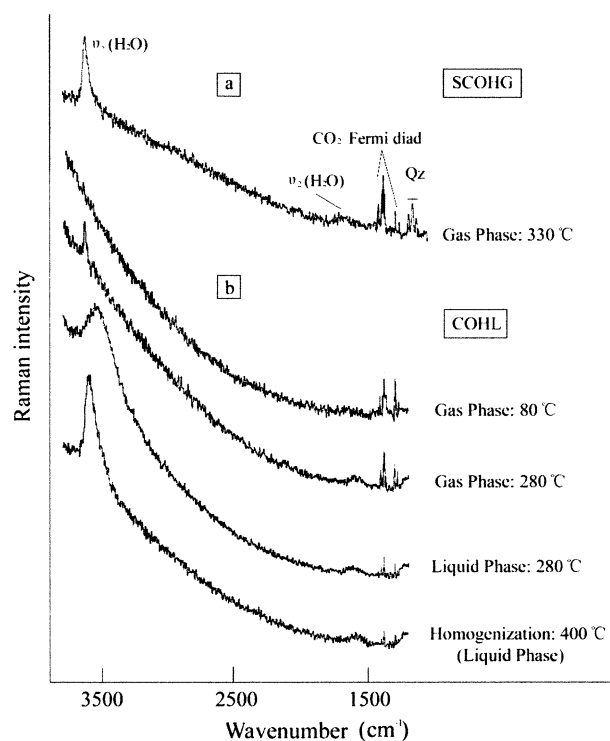


Fig. 2. Raman spectra of synthetic fluid inclusions. (a) SCOHG of the gas phase at 330°C; (b) COHL of different phases and temperatures.

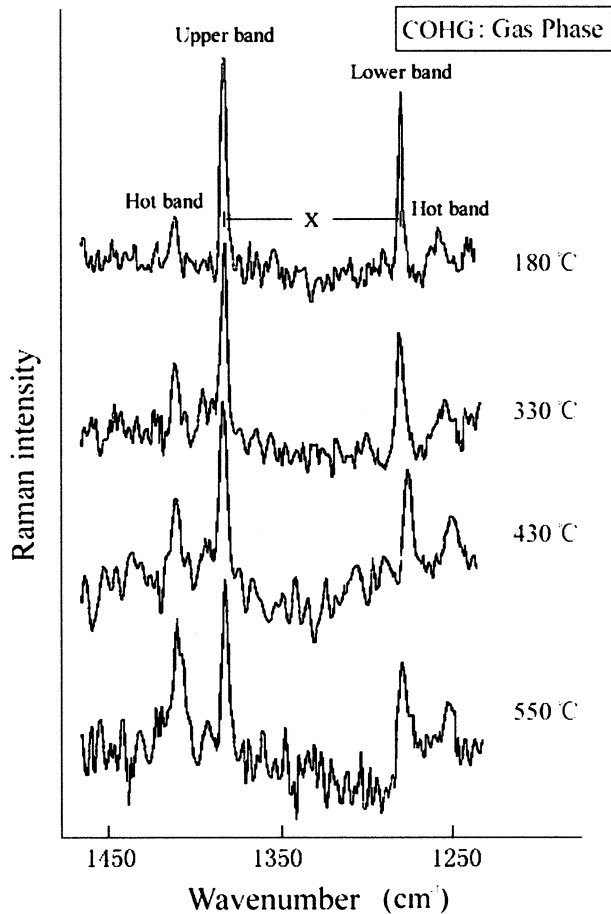


Fig. 3. Raman spectra of CO<sub>2</sub> in the gas phase of COHG at different temperatures. X is the Fermi diad splitting between the upper and lower bands.

intensity ratios of the hot bands to the Fermi diad increase with increasing temperature. For the Fermi diad splitting (X) between the upper and lower bands of CO<sub>2</sub> in the gas phases of COHG and SCOHG (5% NaCl + 10% CO<sub>2</sub> + H<sub>2</sub>O, Th (G) = 530°C), Figure 4 shows that the variations of x values are small at lower temperatures, whereas, with increasing temperature, they present more and more variations.

Water exhibits two Raman bands assigned to internal motions, and they are the bending mode of water ( $\nu_2$ ) around 1600 cm<sup>-1</sup> and a large massif assigned to the stretching vibration ( $\nu_s$ ) in 3000~3700 cm<sup>-1</sup> (Walrafen, 1964, 1967; Ratcliffe and Irish, 1982; Frantz et al., 1993) (Fig. 2). Figure 2b shows that before homogenization, the gas phase gives very weak Raman bands of water, whereas the bands of the liquid phase are very strong, especially for the stretching band. The bending mode of water ( $\nu_2$ ) is weak and has not been studied in this work. As for the very strong spectra of the stretching vibrational mode of water in the liquid phase, with increasing temperature, the massif becomes sharper and sharper, the frequency at maximum intensity ( $\nu_s$ ) shifts to higher wavenumbers, and the full width at half maximum intensity (FWHM) decreases (Fig. 5). When compared with spectra of carbon dioxide, those for the stretching band of water are the ones that exhibit the highest

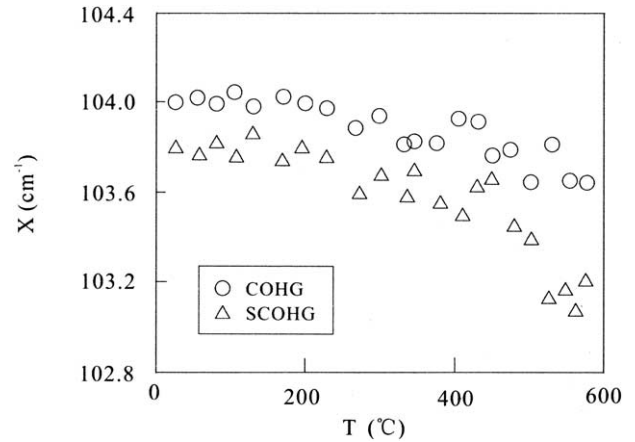


Fig. 4. The Fermi diad splitting (X) between the upper and lower bands of CO<sub>2</sub> in the gas phases of COHG and SCOHG with temperature.

variations in frequency at maximum intensity ( $\nu_s$ ), FWHM, and shape.

Figure 6 illustrates the changes of the  $\nu_s$  and FWHM values of the stretching band of water in the liquid phases for COHL (5% CO<sub>2</sub> + H<sub>2</sub>O, Th (L) = 368°C) and SCOHL (5% NaCl + 5% CO<sub>2</sub> + H<sub>2</sub>O, Th (L) = 400°C) with temperature. It shows that the  $\nu_s$  and FWHM values increase and decrease almost

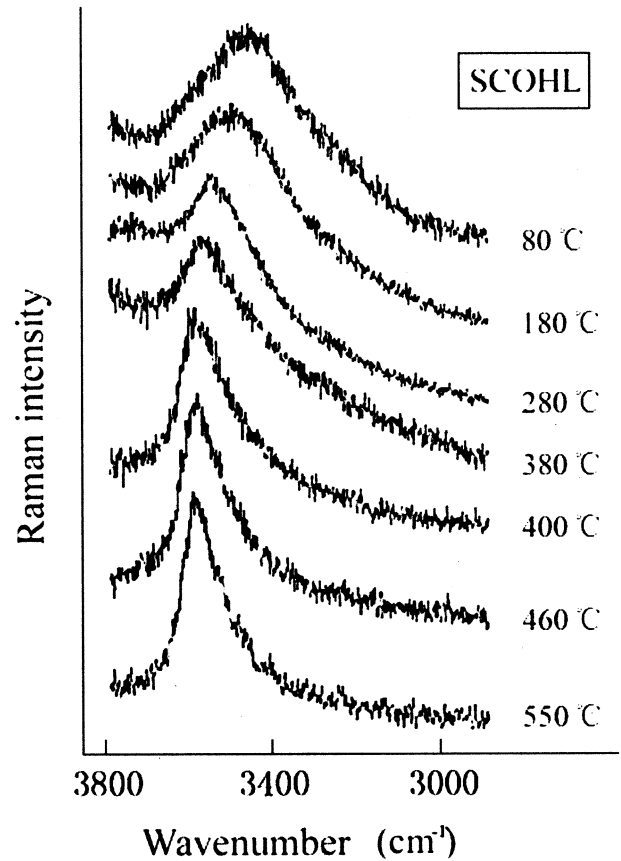


Fig. 5. Raman spectra of the stretching band of water in the liquid phase of SCOHL at different temperatures.

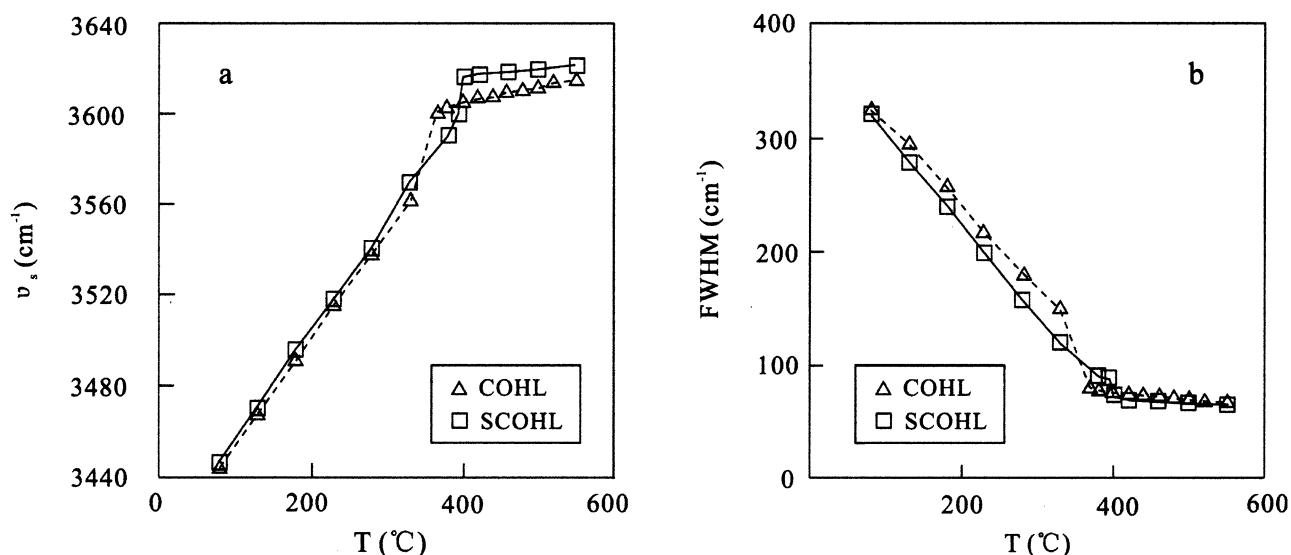


Fig. 6. Variation of  $\nu_s$  and FWHM of the stretching band of water in the liquid phases of COHL and SCOHL with temperature. (a)  $\nu_s$ ; (b) FWHM.

linearly with increasing temperature before homogenization, respectively; near the Th, they both change abruptly; whereas, for the homogeneous liquid phases, the variations of the  $\nu_s$  with temperature are small.

#### 4. DISCUSSION

##### 4.1. Raman Vibration of CO<sub>2</sub>

The Raman spectrum for a homogeneous, free CO<sub>2</sub> phase shows that the Fermi resonance splitting (X) between the upper and lower bands is almost linearly related to the pressure at ambient temperature (Rosso and Bodnar, 1995); whereas most CO<sub>2</sub> in natural fluid inclusions are not homogeneous, free phases, and often mix with aqueous solutions. Therefore, the spectra of carbon dioxide in the gas phase are characterized in this study for COHG (10% CO<sub>2</sub> + H<sub>2</sub>O, Th (G) = 596°C) and SCOHG (5% NaCl + 10% CO<sub>2</sub> + H<sub>2</sub>O, Th (G) = 530°C).

At lower temperatures, water content in gas phases is comparatively low, and its effect can be ignored; therefore, the temperature is regarded to cause the main effect on Raman spectra of carbon dioxide. From the fact that the X values in the gas phases of COHG and SCOHG show small changes with increasing temperature at lower temperatures (Fig. 4), it can be inferred that the temperature has little effect on X at this condition. Therefore, for multiphase, pure CO<sub>2</sub> in fluid inclusions, the densities might be determined through heating to homogeneous gases by Raman spectroscopy as Rosso and Bodnar (1995) did at ambient temperature. At higher temperatures, the X values present very obvious variations; the increase in water content in the gas phases and a nonlinear temperature effect might account for this phenomenon.

The Th of SCOHG of 530°C is lower than that of COHG of 596°C, indicating that at the same temperature the water content in the gas phase of SCOHG is more than that of COHG; as a result, the curve of X values as a function of temperature for SCOHG is lower and with more variations than that for

SCOHG (Fig. 4). When SCOHG becomes a homogeneous gas phase, the abrupt change of X values might mainly result from the significant increase of water and NaCl contents in the gas phase.

Hot bands near the Fermi diad of carbon dioxide are the result of two effects (Rosso and Bodnar, 1995; Dubessy et al., 1999): 1) the anharmonicity of the vibrational levels producing different energetic differences between two successive vibrational levels ( $E[v = 2] - E[v = 1] \neq E[v = 1] - E[v = 0]$ ); and 2) the population of the excited vibrational levels increases with temperature according to the Boltzmann law. Owing to the fact that Fermi resonance doubles the number of hot bands, there are two hot bands near the fundamental bands, at 1380 and 1278 cm<sup>-1</sup>. With increasing temperature, the population of thermally excited vibrational levels increases, therefore, the intensity ratio of the hot bands to the Fermi diad increases (Fig. 3), which indicates that the intensity ratio might be used to estimate temperature, for example, the temperature of an externally heated diamond anvil cell (DAC) can be calibrated by this method.

##### 4.2. Hydrogen Bonding of Water

Owing to the strong H<sub>2</sub>O-H<sub>2</sub>O interactions and the partial weakening of the covalent O-H stretching due to the existence of an O-H-O bridge, the Raman spectrum of the stretching band of water exhibits the highest variations in both frequency at maximum intensity ( $\nu_s$ ) and FWHM. Therefore, we can obtain the changes of the strength of the hydrogen bonding by the variations of the  $\nu_s$  and FWHM (Frantz et al., 1993; Ikushima et al., 1998a). As a result of increasing temperature, the bands of stretching vibration of water become sharper and sharper and the  $\nu_s$  shift to higher wavenumbers (Fig. 5), indicating that the hydrogen bonds decrease with increasing temperature. For the spectra of water in the liquid phases before homogenization, Figure 6 shows that the  $\nu_s$  and FWHM values increase and

decrease almost linearly with increasing temperature, respectively, suggesting that almost linear decreases of hydrogen bonds result from increasing temperature. There are liquid phase and gas phase coexisting before homogenization, so the changes of the pressures in the inclusions are very slight with temperature, and it is assumed to be isobaric, indicating that increasing temperature results in almost linear decreases of the hydrogen bonds on this condition.

Comparing the spectra of the stretching bands of water in the liquid phase of SCOHL (5% NaCl + 5% CO<sub>2</sub> + H<sub>2</sub>O, Th (L) = 400°C) with that of COHL (5% CO<sub>2</sub> + H<sub>2</sub>O, Th (L) = 368°C before homogenization, the  $\nu_s$  and FWHM values of SCOHL lie above and below the corresponding value of COHL, respectively (Fig. 6). The liquid phase of SCOHL contains 5% NaCl, whereas that of COHL contains no NaCl; thus, NaCl might account for the difference of the spectra. During heating of the fluid mixtures in COHL and SCOHL, and as the systems approach the homogenization temperatures, the  $\nu_s$  and FWHM values change abruptly (Fig. 6), indicating a rapid decrease in the hydrogen bonds caused by the significant increase of CO<sub>2</sub> content in the liquid phase during homogenization.

Differing from the great changes of the stretching bands of water in the liquid phases below Th, with increasing temperature, the shape of these bands for the homogeneous liquid phases presents less change, and the variations of the  $\nu_s$  and FWHM values are small (Figs. 5 and 6). It can be assumed that the fluids are isochoric above Th, the changes of the spectra on this condition are slight with increasing temperature, indicating that the interactions of water molecules are slightly affected and the strength of the hydrogen bonding remains almost constant here.

At the maximum temperature of 550°C of this study, the  $\nu_s$  values of COHL and SCOHL are 3614 and 3621 cm<sup>-1</sup> respectively. Compared with the  $\nu_s$  value of 3756 cm<sup>-1</sup> for isolated monomer water (Frantz et al., 1993), these lower values indicate that the interactions of water molecules still exist and a certain extent of the hydrogen bonding network remains at 550°C for these fluids.

## 5. CONCLUSION

At lower temperatures, the variation of Fermi resonance splittings (X) of Raman spectra for carbon dioxide is small only with increasing temperature, so the densities of multiphase, pure CO<sub>2</sub> in natural inclusions might be determined using Raman spectroscopy by heating them to a homogeneous phase as Rosso and Bodnar (1995) did at ambient temperature. The intensity ratios of the hot bands to the Fermi diad increase with temperature, and this provides a useful method for the determination of temperature by Raman spectroscopy.

Increasing temperature results in almost a linear decrease of hydrogen bonds of water at isobaric condition. CO<sub>2</sub> and NaCl present have some effect in destroying hydrogen bonding, and the molecular interaction mechanism of CO<sub>2</sub>-NaCl-H<sub>2</sub>O mixtures should be studied further to reveal the details of the changes of the hydrogen bonding. Our results show that the hydrogen bonds remain close to the temperature of 550°C used in the present study, and therefore, the hydrogen bonds of water

at the temperatures above the critical temperature of water (374°C) can not be ignored.

*Acknowledgments*—The authors wish to deeply thank Prof. Yigang Zhang (Institute of Geology, Chinese Academy of Sciences, Beijing) for help with synthesis of fluid inclusions and Dr. Mouchun He (Department of Geochemistry, China University of Geosciences, Wuhan) for assistance in collecting Raman spectra. We are also very grateful to Drs. C. Romano, I-Ming Chou, and an anonymous reviewer for careful and highly instructive reviews of the manuscript and improving our English. This research was supported by the National Natural Science Foundation of China (Grant No. 10299040), the Chinese Academy of Sciences K. C. Wong Postdoctoral Research Award Fund, and the China Postdoctoral Science Foundation.

*Associate editor:* C. Romano

## REFERENCES

- Anderson A. J., Jayanetti S., Mayanovic R. A., Bassett W. A., and Chou I. M. (2002) X-ray spectroscopic investigations of hydrothermal fluids in the diamond anvil cell: The hydration structure of aqueous La<sup>3+</sup> up to 300°C and 1600 bars. *Am. Miner.* **87**, 262–268.
- Bakker R. J. and Diamond W. D. (2000) Determination of the composition and molar volume of H<sub>2</sub>O-CO<sub>2</sub> fluid inclusions by microthermometry. *Geochim. Cosmochim. Acta.* **64**, 1753–1764.
- Bassett W. A., Anderson A. J., Mayanovic R. A., and Chou I. M. (2000) Hydrothermal diamond anvil cell for XAFS studies of first-row transition elements in aqueous solution up to supercritical conditions. *Chem. Geol.* **167**, 3–10.
- Bellissent-Funel M. C. and Tassaing T. (1997) The structure of supercritical heavy water as studied by neutron diffraction. *J. Chem. Phys.* **107**, 2942–2949.
- Bellissent-Funel M. C. (2001) Structure of supercritical water. *J. Molec. Liquids* **90**, 313–322.
- Bodnar R. J. and Sterner S. M. (1985) Synthetic fluid inclusions in natural quartz. II. Application to PVT studies. *Geochim. Cosmochim. Acta.* **49**, 1855–1859.
- Carey D. M. and Korenowski G. M. (1998) Measurement of the Raman spectrum of liquid water. *J. Chem. Phys.* **108**, 2669–2675.
- Carey D. M., Plesko E. P., and Outwater J. O. (1998) Advanced in situ sapphire test cell for Raman spectroscopy within aqueous environments. *Appl. Spectrosc.* **52**, 958–962.
- Daimon H., Kang K., Sato N., and Fujie K. (2001) Development of marine waste recycling technologies using sub- and supercritical water. *J. Chem. Eng. Jpn.* **34**, 1091–1096.
- Duan Z., Møller N., and Weare J. H. (2003) Equations of state for the NaCl-H<sub>2</sub>O-CH<sub>4</sub> system and the NaCl-H<sub>2</sub>O-CO<sub>2</sub>-CH<sub>4</sub> system: Phase equilibria and volumetric properties above 573 K. *Geochim. Cosmochim. Acta.* **67**, 671–680.
- Dubessy J., Buschaert S., Lamb W., Pironon J., and Thiéry R. (2001) Methane-bearing aqueous fluid inclusions: Raman analysis, thermodynamic modelling and application to petroleum basins. *Chem. Geol.* **173**, 193–205.
- Dubessy J., Moissette A., Bakker R. J., Frantz J. D., and Zhang Y. G. (1999) High-temperature Raman spectroscopic study of H<sub>2</sub>O-CO<sub>2</sub>-CH<sub>4</sub> mixtures in synthetic fluid inclusions: First insights on molecular interactions and analytical implications. *Eur. J. Miner.* **11**, 23–32.
- Ebukuro T., Takami A., Oshima Y., and Koda S. (1999) Raman spectroscopic studies on hydrogen bonding in methanol and methanol/water mixtures under high temperature and pressure. *J. Supercritical Fluids* **15**, 73–78.
- Fournier P., Oelkers E. H., Gout R., and Pokrovski G. (1998) Experimental determination of aqueous sodium-acetate dissociation constants at temperatures from 20 to 240°C. *Chem. Geol.* **151**, 69–84.
- Frantz J. D. (1998) Raman spectra of potassium carbonate and bicarbonate aqueous fluids at elevated temperature and pressures: Comparison with theoretical simulations. *Chem. Geol.* **152**, 211–225.
- Frantz J. D., Dubessy J., and Mysen B. (1993) An optical cell for Raman spectroscopic studies of supercritical fluids and its applica-

- tion to the study of water to 500°C and 2000 bar. *Chem. Geol.* **106**, 9–26.
- Frantz J. D., Dubessy J., and Mysen B. O. (1994) Ion-pairing in aqueous MgSO<sub>4</sub> solutions along an isochore to 500°C and 11 kbar using Raman spectroscopy in conjunction with the diamond-anvil cell. *Chem. Geol.* **116**, 181–188.
- Frost D. J. and Wood B. J. (1997) Experimental measurements of the properties of H<sub>2</sub>O-CO<sub>2</sub> mixtures at high pressures and temperatures. *Geochim. Cosmochim. Acta.* **61**, 3301–3305.
- Furutaka S., Kondo H., and Ikawa S. (2001) Infrared spectroscopic study of water-aromatic hydrocarbon mixtures at high temperatures and pressures. *Bull. Chem. Soc. Jpn.* **74**, 1775–1788.
- Gorbaty Yu E. and Kalinichev A. G. (1995) Hydrogen bonding in supercritical water. I. Experimental results. *J. Phys. Chem.* **99**, 5336–5340.
- Hoffmann M. M. and Conradi M. S. (1997) Are there hydrogen bonds in supercritical water. *J. Am. Chem. Soc.* **119**, 3811–3817.
- Hu S. M., Zhang R. H., and Zhang X. T. (2000) A study of near and supercritical fluids using diamond anvil cell and in-situ FTIR spectroscopy. *Acta Geol. Sinica* **74**, 412–417.
- Ikushima Y., Hatakeda K., Saito N., and Arai M. (1998a) An *in situ* Raman spectroscopy studies of subcritical and supercritical water: The peculiarity of hydrogen bonding near the critical point. *J. Chem. Phys.* **108**, 5855–5860.
- Ikushima Y., Saito N., and Arai M. (1998b) Raman spectral studies of aqueous zinc nitrate solution at high temperatures and at a high pressure of 30MPa. *J. Phys. Chem. B.* **102**, 3029–3035.
- Kritzer P. and Dinjus E. (2001) An assessment of supercritical water oxidation (SCWO): Existing problems, possible solutions and new reactor concepts. *Chem. Eng. J.* **83**, 207–214.
- Marti J. (1999) Analysis of the hydrogen bonding and vibrational spectra of supercritical model water by molecular dynamics simulations. *J. Chem. Phys.* **110**, 6876–6886.
- Marti J. (2000) Dynamic properties of hydrogen-bonded networks in supercritical water. *Phys. Rev. E.* **61**, 449–456.
- Marti J., Padro J. A., and Guàrdia E. (1996) Molecular dynamics simulation of liquid water along the coexistence curve: Hydrogen bonds and vibrational spectra. *J. Chem. Phys.* **105**, 639–649.
- Matubayasi N., Wakai C., and Nakahara M. (1997a) Structural study of supercritical water. I. Nuclear magnetic resonance spectroscopy. *J. Chem. Phys.* **107**, 9133–9140.
- Matubayasi N., Wakai C., and Nakahara M. (1997b) NMR study of water structure in super- and subcritical conditions. *Phys. Rev. Lett.* **78**, 2573–2576.
- Mayanovic R. A., Anderson A. J., Bassett W. A., and Chou I. M. (2001) Hydrogen bond breaking in aqueous solutions near the critical point. *Chem. Phys. Lett.* **336**, 212–218.
- Mitton D. B., Eliaz N., Cline J. A., and Latanision R. M. (2001) An overview of the current understanding of corrosion in SCWO systems for the destruction of hazardous waste products. *Materials Technology* **16**, 44–53.
- Ohtaki H., Radnai T., and Yamaguchi T. (1997) Structure of water under subcritical and supercritical conditions studied by solution X-ray diffraction. *Chem. Soc. Rev.* **26**, 41–51.
- Okada K., Imashuku Y., and Yao M. (1997) Microwave spectroscopy of supercritical water. *J. Chem. Phys.* **107**, 9302–9311.
- Okhulkov A. V. and Gorbaty Y. E. (2001) The pair correlation functions of 1.1 M NaCl aqueous solution at a constant pressure of 1000 bar in the temperature range 20–500 degrees C. *J. Molec. Liquids* **93**, 39–42.
- Postorino P., Tromp R. H., Ricci M. A., Soper A. K., and Neilson G. W. (1993) The interatomic structure of water at supercritical temperatures. *Nature* **366**, 668–670.
- Ramos S., Barnes A. C., Neilson G. W., and Capitan M. J. (2000) Anomalous X-ray diffraction studies of hydration effects in concentrated aqueous electrolyte solutions. *Chem. Phys.* **258**, 171–180.
- Ratcliffe C. I. and Irish D. E. (1982) Vibrational studies of solution at elevated temperatures and pressures. 5. Raman studies of liquid water up to 300°C. *J. Phys. Chem.* **86**, 4897–4905.
- Ricci M. A., Nardone M., and Fontana A. (1998) Light and neutron scattering studies of the OH stretching band in liquid and supercritical water. *J. Chem. Phys.* **108**, 450–454.
- Rosso K. M. and Bodnar R. J. (1995) Microthermometric and Raman spectroscopic detection limits of CO<sub>2</sub> in fluid inclusions and the Raman spectroscopic characterization of CO<sub>2</sub>. *Geochim. Cosmochim. Acta.* **59**, 3961–3975.
- Savage P. E., Gopalan S., Mizan T. I., Martino C. J., and Brock E. E. (1995) Reactions at supercritical conditions: Applications and fundamentals. *AIChE J.* **41**, 1723–1778.
- Schmidt C. and Bodnar R. J. (2000) Synthetic fluid inclusions: XVI. PVTX properties in the system H<sub>2</sub>O-NaCl-CO<sub>2</sub> at elevated temperatures, pressures, and salinities. *Geochim. Cosmochim. Acta.* **64**, 3853–3869.
- Seward T. M., Henderson C. M. B., Charnock J. M., and Driesner T. (1999) An EXAFS study of solvation and ion pairing in aqueous strontium solutions to 300°C. *Geochim. Cosmochim. Acta.* **63**, 2409–2418.
- Shmulovich K. I. and Graham C. M. (1999) An experimental studies of phase equilibria in the system H<sub>2</sub>O-CO<sub>2</sub>-NaCl at 800 and 9 Kbar. *Contrib. Mineral. Petrol.* **136**, 247–257.
- Soper A. K., Bruni F., and Ricci M. A. (1997) Site-site pair correlation functions of water from 25 to 400°C: Revised analysis of new and old diffraction data. *J. Chem. Phys.* **106**, 247–254.
- Stern S. M. and Bodnar R. J. (1984) Synthetic fluid inclusions in natural quartz. I. Compositional types synthesized and applications to experimental geochemistry. *Geochim. Cosmochim. Acta.* **48**, 2659–2668.
- Suleimenov O. M. and Seward T. M. (1997) A spectrophotometric study of hydrogen sulphide ionization in aqueous solutions to 350°C. *Geochim. Cosmochim. Acta.* **61**, 5187–5198.
- Tromp R. H., Postorino P., Neilson G. W., Ricci M. A., and Soper A. K. (1994) Neutron diffraction studies of H<sub>2</sub>O/D<sub>2</sub>O at supercritical temperatures. A direct determination of g<sub>HH</sub>(r), g<sub>OH</sub>(r), and g<sub>OO</sub>(r). *J. Chem. Phys.* **107**, 6210–6215.
- Wallen S. L., Palmer B. J., and Fulton J. L. (1998) The ion pairing and hydration structure of Ni<sup>2+</sup> in supercritical water at 425°C determined by x-ray absorption fine structure and molecular dynamics studies. *J. Chem. Phys.* **108**, 4039–4046.
- Wallen S. L., Palmer B. J., Pfund D. M., Fulton J. L., Newville M., Ma Y., and Stern E. A. (1997) Hydration of bromide ion in supercritical water: An x-ray absorption fine structure and molecular dynamics study. *J. Phys. Chem. A.* **101**, 9632–9640.
- Walrafen G. E. (1964) Raman spectral studies of water structure. *J. Chem. Phys.* **40**, 3249–3256.
- Walrafen G. E. (1967) Raman spectral studies of the effects of temperature on water structure. *J. Chem. Phys.* **47**, 114–126.
- Walrafen G. E., Yang W. H., and Chu Y. C. (1999) Raman spectra from saturated water vapor to the supercritical fluid. *J. Phys. Chem. B.* **103**, 1332–1338.
- Weng K. N., Wang B. S., Xiao W. S., Xu S. P., Lü G. C., and Zhang H. Z. (1999) Experimental study on hydrocarbon formation due to reactions between carbonates and water or water-bearing minerals in deep earth. *Chin. J. Geochim.* **18**, 115–120.
- Weng K. N., Xiao W. S., Zhang H. Z., and Wang B. S. (1997) Experimental probing on formation mechanism of hydrocarbon in deep earth. *China Oil & Gas* **4**, 39–40.
- Wienecke P., Finsterhölzl H., Schrötter H. W., and Brandmüller J. (1986) Raman spectra of carbon dioxide and its isotopic variants in the Fermi resonance region. Part IV: Temperature dependence on Q-branch intensities from 300K to 650K. *Appl. Spectrosc.* **40**, 70–75.
- Xiao W. S., Weng K. N., Lü G. C., and Wang B. S. (2001) Experiments on reaction of polyethylene and water under high pressure and high temperature. *Chin. J. High Press. Phys.* **15**, 169–177 (in Chinese with English abstract).
- Yamaguchi Y., Yasutake N., and Nagaoka M. (2001) Theoretical prediction of proton chemical shift in supercritical water using gas-phase approximation. *Chem. Phys. Lett.* **340**, 129–136.
- Yamanaka J., Mori S., and Kaneko Y. (2001) Hydrothermal synthesis of vanadium-based layered compound with 1 nm basal spacing. *Materials Transactions* **42**, 1854–1857.
- Ziegler K. J., Doty R. C., Johnston K. P., and Korgel B. A. (2001) Synthesis of organic monolayer-stabilized copper nanocrystals in supercritical water. *J. Am. Chem. Soc.* **123**, 7797–7803.
- Zheng H. F., Xie H. S., Xu Y. S., Song M. S., Ge J., and Zhang Y. M. (1997) Study on the electrical conductivity of 0.025mol NaCl solution at 0.25–3.75 GPa and 20–370°C. *Acta Geol. Sinica* **71**, 273–281.